

PFC/JA-95-47

## H-Modes on Alcator C-Mod

J.A. Snipes, A.E. Hubbard, D.T. Garnier,  
S.N. Golovato, R.S. Granetz, M. Greenwald,  
I.H. Hutchinson, J. Irby, B. LaBombard, E.S. Marmor,  
A. Niemczewski, P.J. O'Shea, M. Porkolab, P. Stek,  
Y. Takase, J.L. Terry, R. Watterson, S.M. Wolfe

November, 1995

Submitted to Plasma Physics and Controlled Fusion.

This work was supported by the U. S. Department of Energy Contract No. DE-AC02-78ET51013. Reproduction, translation, publication, use and disposal, in whole or in part by or for the United States government is permitted.

# H-modes on Alcator C-Mod

J A Snipes, A E Hubbard, D T Garnier, S N Golovato, R S Granetz, M Greenwald, I H Hutchinson, J Irby, B LaBombard, E S Marmor, A Niemczewski, P J O'Shea, M Porkolab, P Stek, Y Takase, J L Terry, R Watterson, S M Wolfe

Plasma Fusion Center, Massachusetts Institute of Technology, Cambridge, MA, 02139, USA.

**Abstract.** H-modes exhibiting improved confinement above L-mode are achieved in Alcator C-Mod with ICRF and with ohmic heating alone without boronization. Both ELM-free and ELMy H-modes are obtained with total input power from 0.75 to 4.2 MW over a range of densities ( $0.8$  to  $3 \times 10^{20} \text{ m}^{-3}$ ) and toroidal fields (3 to 8 T). Type III ELMs are often observed to have coherent, high  $m$  and  $n$  precursor oscillations with frequencies of 100 - 160 kHz. The threshold power required to achieve H-mode increases with density and toroidal field, in rough agreement with scalings derived from other tokamaks. The power densities and density times toroidal field products are an order of magnitude larger than in other tokamaks, in the range of values expected for ITER. The L-H and H-L transitions occur at approximately the same edge electron temperature. A low density limit to the H-mode is found at about  $8 \times 10^{19} \text{ m}^{-3}$ . A high midplane neutral pressure limit of about 0.6 mTorr is also observed.

## 1. Introduction

The improved particle and energy confinement regime called H-mode [1,2] is extended on the compact, high field divertor tokamak, Alcator C-Mod [3], up to toroidal fields and power densities never before attained. H-modes have been achieved on Alcator C-Mod at toroidal fields of nearly 8 T and average surface power densities of nearly  $0.6 \text{ MW/m}^2$ . All H-modes have occurred with the ion  $\nabla B$  drift in the favorable direction [2] toward a single null X point. Attempts were made to achieve H-modes with the ion  $\nabla B$  drift direction away from the single null X point by reversing both the plasma current and the toroidal field, but no H-modes were observed with up to 4.5 MW of input power. All H-mode plasmas were deuterium. Unlike most other divertor tokamaks, which have graphite first walls, Alcator C-Mod has an all molybdenum first wall and has achieved all of these H-modes without boronization. Usually, only one to two hours of Electron Cyclotron Discharge Cleaning (ECDC) in deuterium or helium is performed before each run. An attempt to condition the walls by injecting 40 lithium pellets throughout the day had no clear effect on the H-mode performance.

Ohmic H-modes have been achieved with plasma currents of  $0.6 < I_p < 0.9 \text{ MA}$  and toroidal fields from  $2.9 < B_T < 5.3 \text{ T}$ . The ohmic input power required to reach H-mode has varied from 0.75 MW to 1.5 MW. ELM-free ohmic H-modes occur for toroidal fields less than 3.7 T with maximum durations of about 0.14 sec. Energy confinement times up to 80 msec have been obtained in ELM-free ohmic H-modes. At higher field, up to 5.3 T, only ELMy ohmic H-modes have been observed with durations up to 0.46 sec.

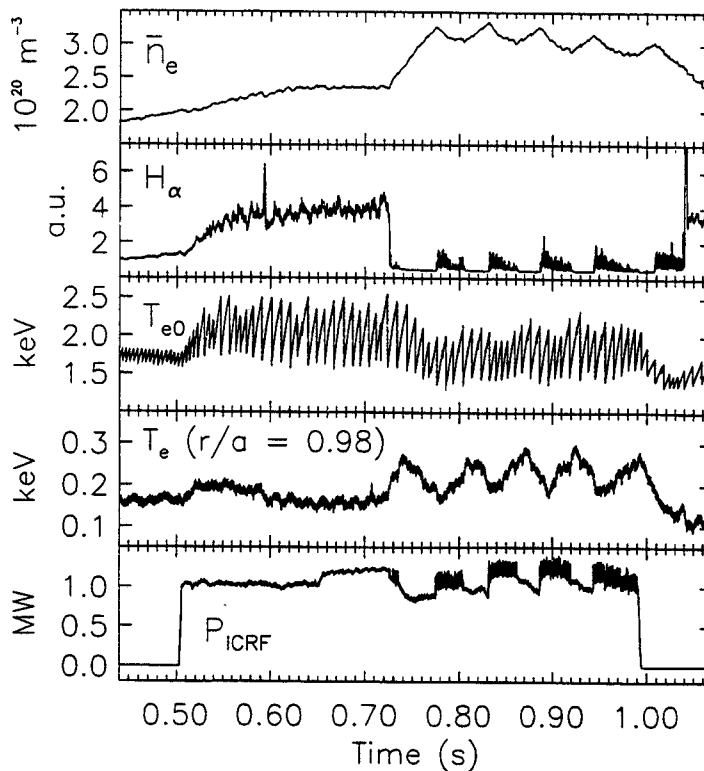


**Figure 1.** ICRF H-mode discharge showing the line averaged density, midplane  $H_{\alpha}$  emission, central and edge  $T_e$ , and the ICRF power. Large sawtooth oscillations are visible on the central  $T_e$  during ICRF heating.

ICRF heated H-modes have been achieved at toroidal fields of 5.3 and 7.9 T, corresponding to the cyclotron resonance for H and  $He^3$  minorities at the 80 MHz fixed frequency of the ICRF transmitters. The total input power for ICRF H-modes has varied from 0.9 to 4.2 MW. The maximum duration for ELM-free ICRF H-modes has been limited to about 0.06 sec by increases in density and radiated power as well as by changes in RF coupling that reduce the RF power during the ELM-free phase. Figure 1 shows an example of an ICRF heated H-mode discharge just above threshold. The outer gap must be maintained less than 3 cm to couple the RF power and the average value was 1.7 cm. The density and temperature scrape off lengths are typically 0.5 to 1 cm. Energy confinement times up to 55 msec have been obtained in ELM-free ICRF H-modes. The H-modes at 7.9 T occurred shortly after a lithium pellet was injected into the plasma, before the density returned to the pre-pellet level. Similar discharges without pellets showed no signs of H-mode. Strong ICRF heating just after the pellet also produces enhanced neutron rates during very peaked density profiles in a kind of P mode [4] or PEP mode [5, 6], suggesting that the lithium has transiently improved wall conditions or that a peaked density profile may be favorable for achieving H-mode.

The operational range of Alcator C-Mod extends the global H-mode database [7] in size, density, toroidal field, and power density. Previous H-mode results on JT60-U [8] and TFTR [9] had toroidal fields up to 4.2 and 5.2 T, surface power densities up to 0.16 and 0.3 MW/m<sup>2</sup>, input powers up to 25 and 28 MW, and line averaged densities up to 0.3 and 0.25 x 10<sup>20</sup> m<sup>-3</sup>, respectively. The results presented here extend the toroidal field

by 50%, the power density by a factor of two, and the electron density by an order of magnitude, into the range expected for ITER [10]. The topics of this paper include an analysis of ELM precursors, a comparison of edge electron temperature and density profiles in L and H-mode, and a study of the parameters that affect the H-mode threshold.

## 2. Edge Localized Modes

Usually, the Edge Localized Modes (ELMs) [11] on Alcator C-Mod are regular periodic spikes on the  $H_\alpha$  emission known as Type III ELMs [12] with the characteristic that the repetition rate decreases with increasing input power. In ohmic plasmas with input power between 0.7 and 1.1 MW, the ELM repetition rate varies from 6 to 3 kHz, while in ICRF heated plasmas with 1.5 to 4 MW of input power, the repetition rate varies from 4 to about 1 kHz. However, under some conditions, the ELMs become very small and irregular in shape on the  $H_\alpha$  emission with repetition rates below 1 kHz at all power levels. Despite their small amplitude, well below the L-mode  $H_\alpha$  level (Fig. 1), they degrade confinement twice as much as the regular Type III ELMs.

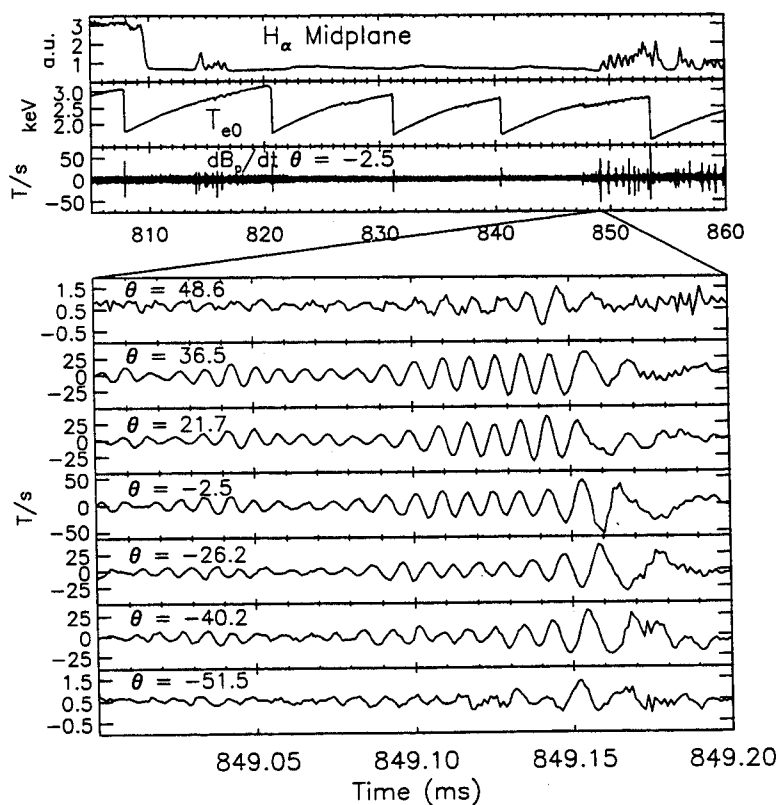


**Figure 2.** ICRF H-mode discharge showing the midplane  $H_\alpha$  emission, central  $T_e$ , the ICRF power, and an array of fast poloidal field pick-up coil signals. An expanded view of high frequency ELM precursor oscillations on the outboard limiter coils shows how the phase varies strongly with poloidal angle.

Both the ohmic and ICRF ELMs have coherent precursor oscillations that are visible on several arrays of fast poloidal field pick-up coils located on the outboard limiters about 6 to 8 cm from the plasma, typically. The frequency of the precursors

varies from 100 to 160 kHz. The growth rates at 8 T appear to be faster than at lower field in that the ELM occurs after about two oscillations, while at lower field four to six oscillations are typical. Figure 2 shows an example of a discharge with particularly clear coherent ELM precursor oscillations. With arrays of seven fast poloidal field pick-up coils on each side of one outboard limiter and four pick-up coils on each side of another outboard limiter nearly 180° away toroidally, it is possible to estimate the  $m$  and  $n$  numbers of the dominant MHD mode. The pick-up coil signals are sampled at 1 MHz. The mode rotation is generally in the electron diamagnetic drift direction. By measuring the slope of the phase of the oscillations versus the poloidal position along the outboard limiter, only a lower limit on the poloidal mode number can be determined, since the phase cannot be followed around the entire poloidal circumference. This estimate gives  $m > 10$ , assuming that the phase will vary faster on the inboard side of the machine, as has been observed on JET [13]. Similarly, toroidal mode numbers from  $n > 5$  to 15 have been estimated from the measured phase difference of coil signals from opposite sides of each outboard limiter. While the phase appears to be coherent on signals from opposite sides of each limiter, with a toroidal separation of  $\phi = 9^\circ$ , the signals from coils separated by  $\phi = 146^\circ$  or  $164^\circ$  are uncorrelated. To determine the  $m$  and  $n$  numbers more precisely, measurements with higher spatial and temporal resolution are required.

### 3. Edge Profile Measurements

Measurements of the electron density and temperature are made with a fast scanning Langmuir probe array [14], two flush mounted divertor Langmuir probe arrays, a five channel O-mode AM reflectometer [15], a four channel Thomson scattering system [16], and two electron cyclotron emission (ECE) diagnostics, a Michelson interferometer and a nine channel grating polychromator [17]. The Langmuir probes provide electron density and temperature profiles outside the last closed flux surface (LCFS), while the reflectometer, Thomson scattering diagnostic and ECE polychromator provide electron density and temperature profiles inside the LCFS. The fast scanning probe (FSP) is an array of four directional probes that is rapidly inserted and withdrawn from the plasma in 100 msec at an upstream location from the flush mounted probes (FMP) in the divertor plates. It is limited to measurements outside the LCFS to avoid overheating the probe. The reflectometer channels have fixed frequencies corresponding to cutoff densities that range from 0.3 and  $1.5 \times 10^{20} \text{ m}^{-3}$ , which provide measurements well into the steep edge gradient region inside the LCFS. During the past run period the Thomson scattering diagnostic had three to four vertical positions across the plasma out to  $r/a \approx 0.87$ . The ECE polychromator, which is cross-calibrated against the Michelson, provides high time resolution (50  $\mu\text{s}$ ) and radial resolution ( $\sim 1$  cm) measurements deep into the plasma. The radial spacing between channels depends on the grating chosen and the toroidal field, but is typically about 2.5 cm with channels out to  $r/a \approx 0.98$ . Edge temperature measurements by ECE are limited by the optical depth of the plasma, which was typically between 1 and 3 at  $\psi=0.95$  for the discharges studied here. Instrumental crosstalk on the polychromator allowed a small percentage of 3rd harmonic radiation from the plasma center to be received on the outer channel. These limitations might affect the absolute values of the edge temperatures quoted here by up to 25%, but they will not change the trends observed significantly.

Figure 3a shows profiles of the electron density from the FSP and the FMP during an ohmic discharge shortly before an L-H transition and during an ELMy ohmic H-mode. The density is lower everywhere outside the LCFS during the H-mode. Figure 3b shows the electron temperature profile for the same times, which is also lower outside the LCFS during the H-mode. Near the LCFS, the density gradient sharply increases at an L-H transition as measured by the reflectometer and corroborated by the Thomson scattering diagnostic (Fig. 4). The steep density gradient of  $1 \times 10^{22} \text{ m}^{-4}$  develops in less than 0.5 msec. The electron temperature also increases near the edge during the H-mode as shown in Figure 5. The drop in density and temperature outside the LCFS together with the increase inside clearly demonstrates the steepening of the edge gradients between L and H-mode.

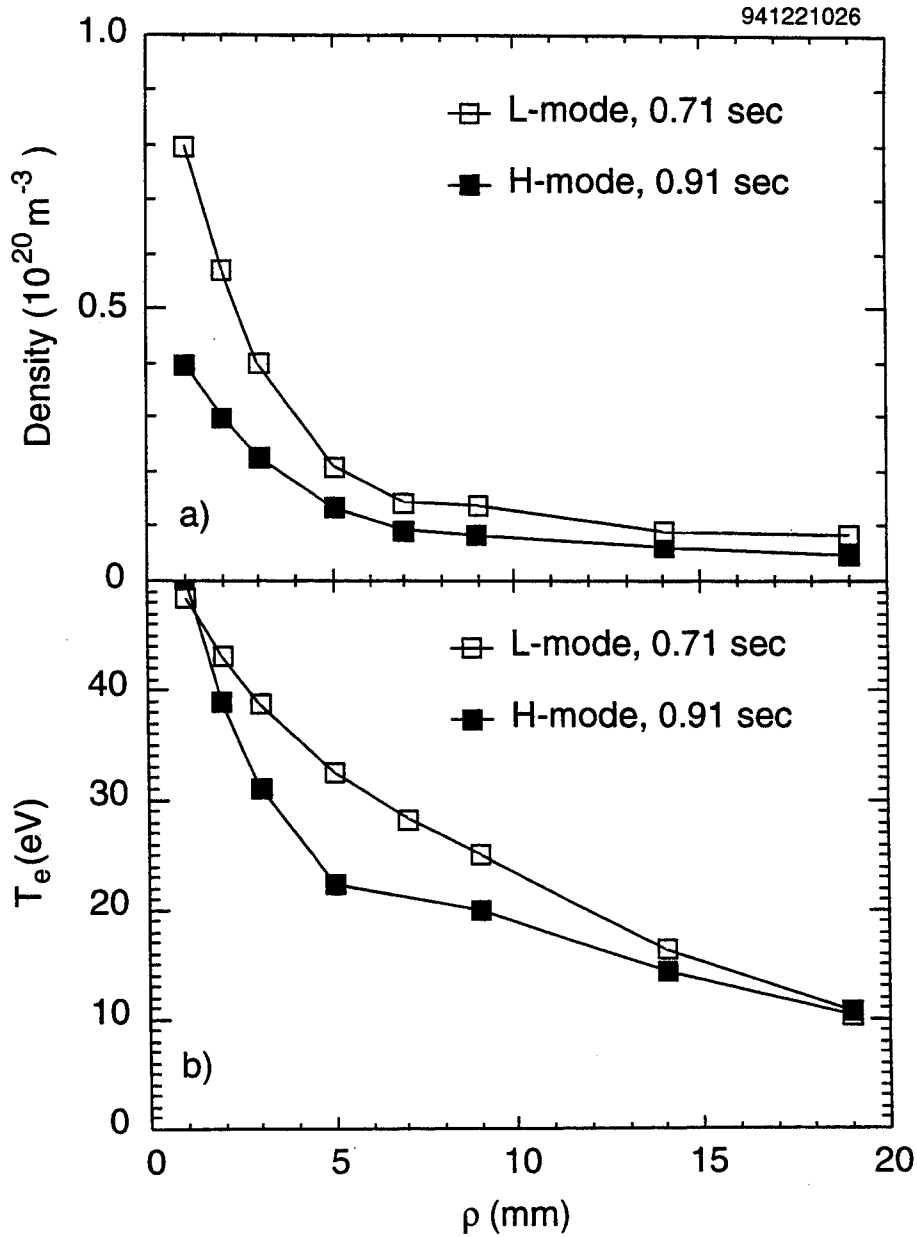


**Figure 3.** Fast Scanning Probe and Flush Mounted Probe a) electron density and b) temperature profiles of the plasma scrape off layer in L and ELMy ohmic H-mode.

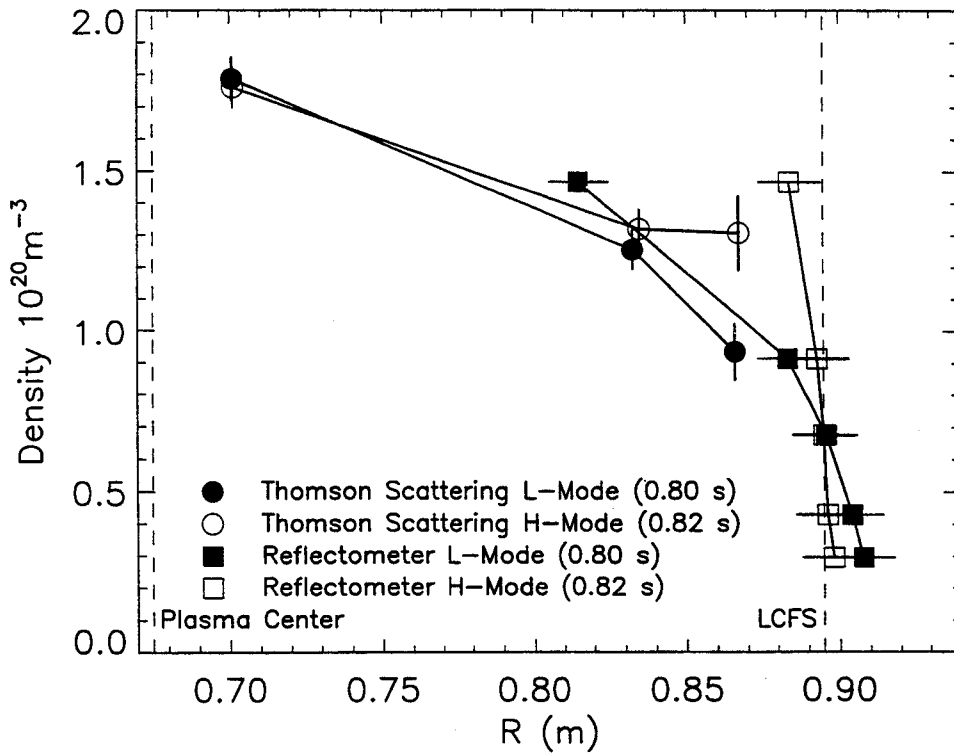


**Figure 4.** Electron density profiles from the Thomson scattering diagnostic and reflectometer in ICRF heated L-mode and ELM-free H-mode.

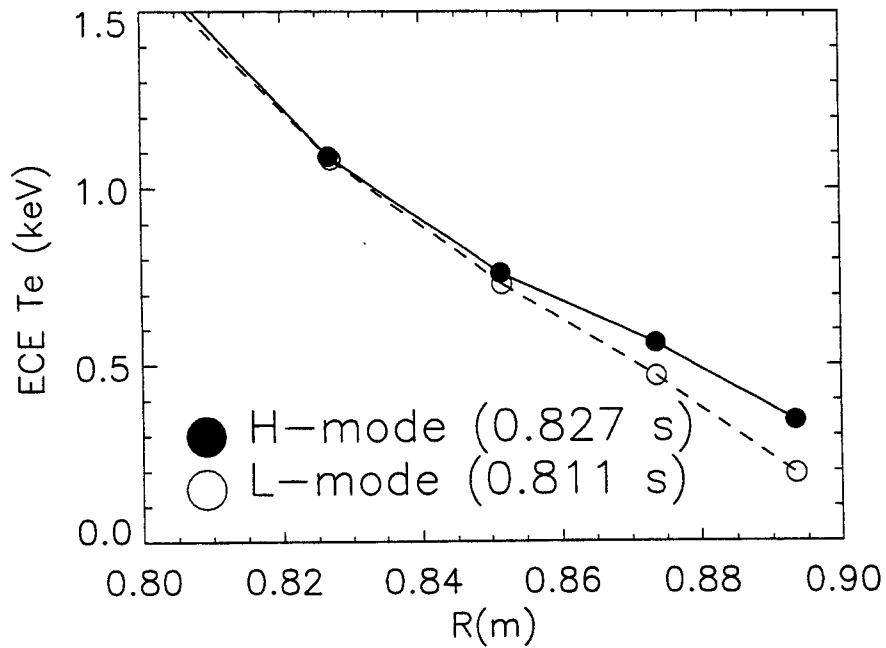


**Figure 5.** Electron temperature profiles from the ECE grating polychromator in L and H-mode. Both profiles are taken just before a sawtooth collapse. The edge region is expanded to clearly show the difference in the edge temperature between L and H-mode. This is the same ICRF heated discharge as in Figure 4.

#### 4. H-mode power threshold

The total input power required to enter the H-mode depends on a number of plasma parameters and machine conditions including the magnetic configuration, wall conditions, electron density, and the toroidal field. The scaling,  $P/S = 0.044 \bar{n}_e B_T$ , where  $P$  is the total input power and  $S$  is the total plasma surface area at the last closed flux surface, was proposed to describe ASDEX-Upgrade [18]. A similar scaling was previously found on DIII-D [19]. Figure 6a shows the scaling for the Alcator C-Mod data taken just before the L-H transition. The data lie between the ASDEX-Upgrade scaling and about a factor of two lower. This may indicate a stronger size scaling. The unique range of the Alcator C-Mod data, together with data from eight other tokamaks, has recently led the ITER H-mode Database Working Group to the scaling,  $P_{\text{thresh}} = 0.3 \bar{n}_e B_T R^{2.5}$  [7]. Since the  $R$  variation is small, no distinction can be drawn in the size scalings from the Alcator C-Mod dataset alone.

Figure 6b shows that the threshold power increases with density and that there is a low density limit at about  $8 \times 10^{19} \text{ m}^{-3}$ . Given the scatter in the data, it is difficult to determine the precise exponent on the density, but it could well be linear. While other machines report H-modes down to line averaged densities of  $2.5 \times 10^{19} \text{ m}^{-3}$  [7], the low density limit on Alcator C-Mod is considerably higher. It has been proposed that hard x rays from runaway electrons, the absence of sawteeth, or locked modes may be

causes for the low density limit. However, in several discharges, where runaways and locked modes were not present and sawteeth were present, the low density limit remained. The minimum threshold power is obtained at densities somewhat above the low density limit, which for ohmic H-modes at 3.5 T was 0.75 MW and for ICRF H-modes at 5.3 T was 1.2 MW. These threshold powers compare very well with the recent scaling found on JT60-U [20],  $P_{\text{th}} = 0.34 R^{1.4} a^{0.4} B_T^{1.5}$ , where  $P_{\text{th}}$  is the power at the optimum density, which gives values of 0.71 and 1.34 MW, respectively.

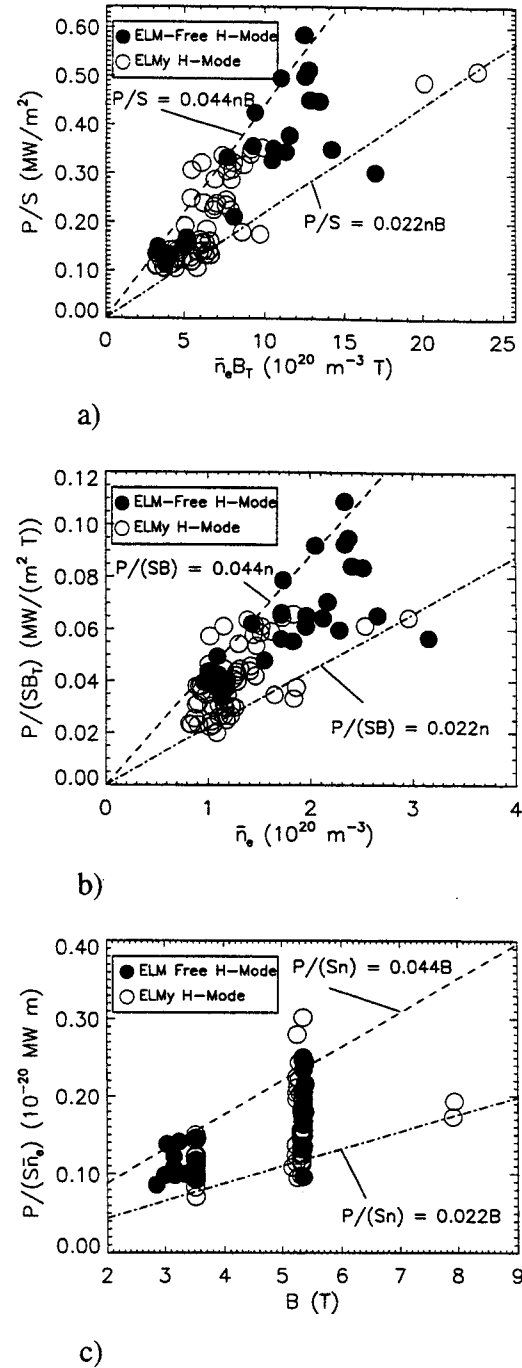


**Figure 6.** Alcator C-Mod data just before transition to H-mode showing a) the dependence on the product  $\bar{n}_e B_T$ , b) on  $\bar{n}_e$ , and c) on  $B_T$ .



Figure 6c shows that the H-mode power threshold increases with toroidal field. However, given the scatter and the limited amount of data at high field, it is not yet possible to distinguish between a linear or square root  $B_T$  dependence. More data is needed at high field to determine the toroidal field dependence. Still, the scatter in the data indicates that there are other parameters besides the line averaged electron density and toroidal field that influence the power threshold.

The midplane neutral pressure appears to influence the H-mode threshold in that no H-modes occur when the midplane neutral pressure exceeds about 0.6 mTorr. This can occur at high density, above about  $2 \times 10^{20} \text{ m}^{-3}$ , when the outer gap is less than about 2 cm. When the divertor is detached, the midplane neutral pressure usually exceeds 0.6 mTorr [21]. Thus, so far, it has not been possible to combine the H-mode in Alcator C-Mod with the detached divertor regime.

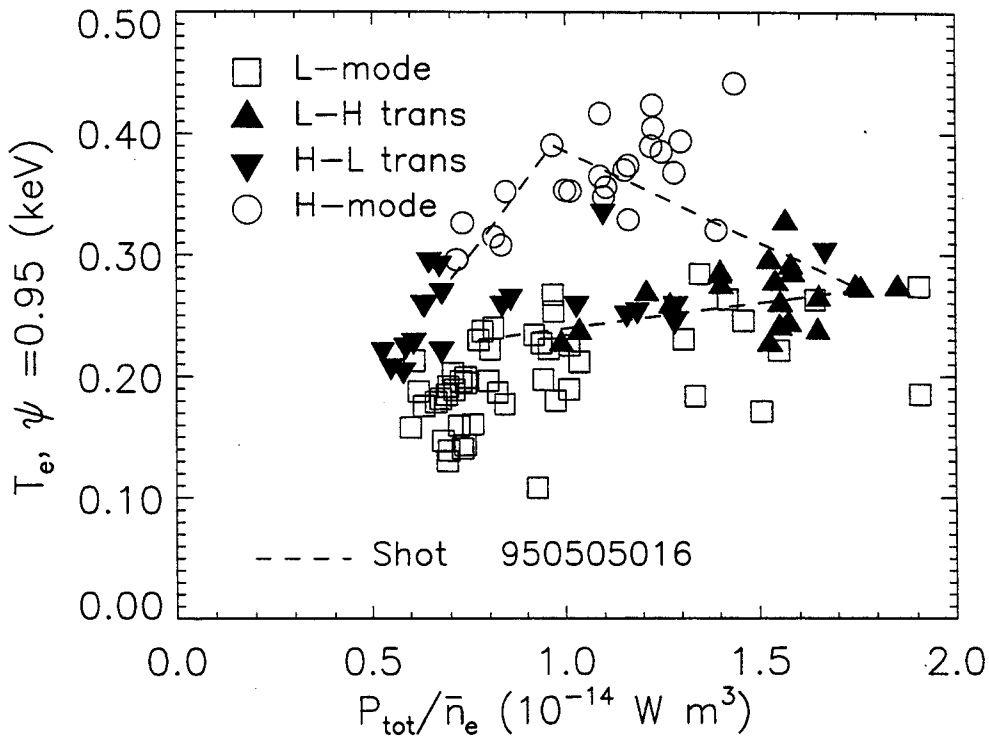


**Figure 7.** Electron temperature at the 95% flux surface versus the ratio of the total input power and the line averaged electron density showing that the L-H and H-L transitions occur at the same edge  $T_e$ . The dashed line follows a typical discharge through the L-mode, L-H transition, H-mode, and H-L transition.

Another parameter that correlates well with the H-mode threshold is the electron temperature in the plasma edge, inside the last closed flux surface. Figure 7 shows  $T_e$  at the 95% flux surface versus the ratio of the total input power to the line averaged density for a number of plasma discharges with  $B_T = 5.3 \text{ T}$  and  $I_p = 1.0 \text{ MA}$ . Different symbols indicate L-mode, H-mode, or just before L-H and H-L transitions. In the L-mode, the edge  $T_e$  increases somewhat with  $P_{\text{tot}}/\bar{n}_e$ , but there appears to be a saturation at high

P/n. A striking feature is that the L-H transition generally occurs when  $T_e(0.95)$  is in the range  $280 \pm 40$  eV. After the transition, the edge temperature increases to typically 400 eV, presumably due to improved thermal confinement. As the density keeps increasing, the edge temperature falls and when it drops back below 280 eV, the H-L transition occurs. Similar edge temperature thresholds (100 - 250 eV) were found in DIII-D [19] and ASDEX [11]. Since the L-H and H-L transitions occur at about the same edge electron temperature, it appears that maintaining the edge temperature may be a necessary if not sufficient condition for maintaining the H-mode. Since reliable temperature measurements in the steep gradient region between  $0.95 < \psi < 1$  are unavailable in Alcator C-Mod, it cannot be ruled out that the H-mode threshold is more directly related to the temperature closer to the LCFS or to the temperature gradient.

A similar variation of L and H-mode edge temperatures is found for other plasma currents, but the transition temperature at the 95% flux surface increases with  $I_p$ . At  $I_p = 0.6$  MA and 5.3 T, no H-modes were observed. This might be due to the colder edge temperatures in L-mode, which never approached the threshold found for higher currents. Below 3.6 T, however, ohmic H-modes do occur with  $I_p \approx 0.6$  MA, but the edge temperature measurements were unavailable. For the few H-modes produced at 8 T and 1 MA, the transition temperatures were somewhat higher than at 5.3 T. A positive dependence of the threshold temperature with field would be consistent with the global power scaling and with DIII-D results [19]. However, the DIII-D results predicted an edge temperature threshold of 115 eV/T, which is higher than on Alcator C-Mod. More data are required to establish this scaling on Alcator C-Mod.

## 5. Conclusions

Detailed measurements of high frequency coherent ELM precursor oscillations show that they have very high m and n numbers. The H-mode threshold power increases with toroidal field and electron density, but also shows a clear correlation with the edge electron temperature. The plasma enters and leaves H-mode at approximately the same value of edge temperature, suggesting that maintaining a given value of the edge temperature may be necessary to remain in H-mode. H-modes do not occur when the midplane neutral pressure exceeds about 0.6 mTorr. While the H-mode threshold can be described in broad terms with global parameters, there are covariances with local parameters that suggest that a scaling based on local parameters may be necessary to provide a more accurate prediction for future devices. A comparison of local thresholds from different experiments would help to determine the appropriate scaling and aid in understanding the physics involved.

## Acknowledgments

We would like to thank the rest of the Alcator team for their excellent engineering and technical support without which this work would not have been possible. This work was supported by U. S. Department of Energy Contract DE-AC02-78ET51013.

## References

- [1] Wagner F, Becker G, Behringer K, Campbell D, Eberhagen A., Engelhardt W, Fußmann G, *et al*, 1982 *Phys. Rev. Lett.* **49** 1408.
- [2] ASDEX Team, 1989 *Nuclear Fusion* **29** 1959.
- [3] Hutchinson I H, Boivin R, Bombarda F, Bonoli P, Fairfax S, Fiore C, Goetz J, *et al*, 1994 *Phys. Plasmas* **1** 1511.
- [4] M. Greenwald, D. Gwinn, S. Milora, J. Parker, R. Parker, S. Wolfe, M. Besen, *et al*, *Phys. Rev. Lett.* **53**, 352 (1984).
- [5] Tubbing, B J D, *et al*, 1991 *Nuclear Fusion* **31** 839.
- [6] Takase Y, Boivin R, Bombarda F, Bonoli P, Fiore C, Garnier D, *et al*, 1995 *Proc. 22nd EPS Conference on Controlled Fusion and Plasma Physics, Bournemouth*, to be published.
- [7] H-Mode Database Working Group, 1994 *Proc. 21st EPS Conference on Controlled Fusion and Plasma Physics, Montpellier* **18B** Part I, 334.
- [8] Kikuchi M, Shirai H, Takizuka T, Kamada Y, Koide Y, Yoshida H, Naitou O, *et al*, 1993 *Plasma Physics and Controlled Nuclear Fusion Research Proc. 14th Int. Conf. Würzburg 1992, IAEA Vienna* **1** 189.
- [9] Bush, C E, Bretz N L, Fredrickson E D, McGuire K M, Nazikian R, Park H K, Schivell J, *et al*, 1991 *Plasma Phys. and Cont. Nuclear Fusion Research Proc. 13th Int. Conf. Washington 1990, IAEA Vienna* **1** 309.
- [10] ITER Joint Central Team, 1993 *Plasma Phys. Control. Fusion* **35** B23.
- [11] Keilhacker M, Becker G, Bernhardt K, Eberhagen A, ElShaer M, Fußmann G, Gehre O, *et al*, 1984 *Plasma Physics and Controlled Fusion* **26** 49.
- [12] Doyle E J, Burrell K H, Lehecka T, Luhmann N C Jr, Matsumoto H, Osborne T, Peebles W A, Philipona R, and Rettig C, 1991 *Proc. 18th EPS Conference on Controlled Fusion and Plasma Physics, Berlin* **15C** Part I, 285.
- [13] Malacarne M, Cripwell P, Duperréx P-A, Edwards A W, Gill R D, Granetz R S, Simonet F, Snipes J, and Weller A, 1987 *Plasma Physics and Controlled Fusion* **29** 1675.
- [14] LaBombard B, Goetz J, Kurz C, Jablonski D, Lipschultz B, McCracken G, Niemczewski A, *et al*, 1995 *Phys. Plasmas* **2** 2242.
- [15] Stek P C and Irby J H, 1994 *Bull. Am. Phys. Soc.* **39** 1667.
- [16] Watterson R, Casey J A, Hubbard A, O'Shea P J, Rollins E, Tambini F, and Giovannozzi E, 1995 *Bull. Am. Phys. Soc.* **40** in press.
- [17] Hubbard A E, Hsu T C, and O'Shea P J, 1995 PFC Report PFC/JA-95-11; O'Shea P J, Hubbard A E, and the Alcator C-Mod Group, 1995 PFC Report PFC/JA-95-11, to be published in *Proc. 9th Joint Workshop on Electron Cyclotron Emission and Electron Cyclotron Resonance Heating*, Borrego Springs, CA.
- [18] Ryter F, Gruber O, Büchl K, Field A R, Fuchs C, Gehre O, Herrmann A, *et al*, 1993 *Proc. 20th EPS Conf. Lisbon* **17C** Part I 23.
- [19] Carlstrom T N, Shimada M, Burrell K H, DeBoo J, Gohil P, Groebner R, Hsieh C, Matsumoto H, and Trost P, 1989 *Proc. 16th EPS Conf. on Cont. Fusion and Plasma Phys., Venice* **13B** Part I, 241
- [20] JT-60 Team, 1995 *Plasma Phys. and Cont. Nuclear Fusion Research Proc. 15th Int. Conf. Seville 1994, IAEA Vienna*, to be published.
- [21] Niemczewski A, PhD Thesis, 1995 *Neutral Particle Dynamics in the Alcator C-Mod Tokamak*, Massachusetts Institute of Technology.